EJNMMI Radiopharmacy and Chemistry

RESEARCH ARTICLE Open Access

SPECT/CT imaging of EGFR-positive head and neck squamous cell carcinoma patient-derived xenografts with ^{203}Pb-PSC-panitumumab in NRG mice

Nasim Sarrami[1], Bryce Nelson[2], Samantha Leier[2], John Wilson[2], Conrad Chan[3], Jalna Meens[4], Teesha Komal[5], Laurie Ailles[4,6], Melinda Wuest[2], Michael Schultz[7], Afsaneh Lavasanifar[1], Raymond M. Reilly[3,4] and Frank Wuest[1,2,8,9*]

*Correspondence:
wuest@ualberta.ca

[1] Faculty of Pharmacy and Pharmaceutical Sciences, University of Alberta, Edmonton, Canada
[2] Department of Oncology, Cross Cancer Institute, University of Alberta, 11560- University Avenue, Edmonton, AB T6G 1Z2, Canada
[3] Leslie Dan Faculty of Pharmacy and Department of Pharmaceutical Sciences, University of Toronto, Toronto, Canada
[4] Princess Margaret Cancer Centre, Toronto, Canada
[5] STTARR Innovation Centre, University Health Network, Toronto, Canada
[6] Department of Medical Biophysics, University of Toronto, Toronto, Canada
[7] Viewpoint Molecular Targeting, Inc, Coralville, IA, USA
[8] Department of Chemistry, University of Alberta, Edmonton, Canada
[9] Cancer Research Institute of Northern Alberta, University of Alberta, Edmonton, Canada

Abstract

Background: The objective of this research was the development and evaluation of ^{203}Pb-labelled panitumumab (^{203}Pb-PSC-panitumumab) as an immuno-SPECT radioligand for the detection of EGFR + head and neck squamous cell carcinoma (HNSCC) in a patient-derived xenograft (PDX) mouse model. The 51.9 h physical half-life and favourable γ-emission (279 keV; 81%) of ^{203}Pb offer an excellent opportunity for developing immuno-SPECT radioligands. Moreover, ^{203}Pb has a complementary therapeutic radionuclide (^{212}Pb), making ^{203}Pb and ^{212}Pb an ideal matched radiotheranostic pair.

Results: Radiolabeling of panitumumab was performed at a pH of 5.0 and room temperature for 5–10 min with [^{203}Pb]Pb(OAc)$_2$, and the incorporation efficiency was determined using radio-TLC. ^{203}Pb-PSC-panitumumab (~ 10 MBq, 140 µl of saline) was injected into the tail vein of NRG mice bearing subcutaneous (s.c.) HNSCC patient-derived xenografts (PDX). SPECT/CT images were acquired at 48 and 120 h post-injection. For biodistribution studies, mice were euthanized five days after ^{203}Pb-panitumumab injection. The tumour and normal tissues were collected and weighed, and uptake of ^{203}Pb was measured in a γ-counter. The uptake was calculated as the percent injected dose per gram of each tissue (ID%/g). Blocking experiments were performed by pretreating a group of mice (n = 5) with 1 mg of panitumumab 1 h before administering ^{203}Pb-PSC-panitumumab. 4–5 chelators of a new lead-specific chelator (PSC) were attached per antibody; radiolabeling efficiency was 99.2 ± 0.7%. The isolated radiochemical yield of ^{203}Pb-PSC-panitumumab was 41.4 ± 8% (n = 5), and the molar activity was 1.2 ± 0.35 GB/mg. SPECT imaging and biodistribution confirmed high accumulation and retention of ^{203}Pb-PSC-panitumumab in the tumour (26% ID/g) at 120 h post-injection (p.i.), which could be reduced to 6.2%ID/g at 120 h p.i. by predosing with panitumumab (1 mg) confirming EGFR specificity of ^{203}Pb-PSC-panitumumab uptake.

Conclusions: Panitumumab was successfully and reproducibly labelled with ^{203}Pb in high radiochemical purity using the chelator PSC-NCS. ^{203}Pb-PSC-panitumumab was specifically accumulated and retained in EGFR + tumours in NRG mice with s.c. HNSCC PDX. ^{203}Pb-PSC-panitumumab is a suitable immuno-SPECT radioligand for imaging EGFR + tumours and has great potential for combining with ^{212}Pb-PSC-panitumumab in a radiotheranostic strategy for imaging and treating HNSCC.

Keywords: Panitumumab, Pb-203, Single-Photon Emission Computed Tomography (SPECT), Epidermal growth factor receptor (EGFR), Radiotheranostics, Pb-212

Introduction

Targeted radionuclide therapy (TRT) is a widely used cancer treatment option that employs radiopharmaceuticals to target and deliver ionizing radiation to kill cancer cells (Li et al. 2020; Sun et al. 2022; Chan et al. 2020). TRTs have been used for cancer therapy, demonstrating increased overall survival as exemplified in patients with thyroid cancer, prostate cancer, and neuroendocrine tumours (Kerr et al. 2022). As a promising type of current cancer therapy, TRT delivers a therapeutic dose of radiation to cancer cells using radioactive drugs (radiopharmaceuticals) labelled with alpha(α)- or beta(β^-)-emitting radioisotopes (Chan et al. 2020; Gill et al. 2017). TRT with α emitters (α-TRT) offers several advantages compared to β^- emitters, mainly due to the delivery of high-energy α-particles (5–9 MeV) to the tumour with a short pathlength (50–100 μm) and high linear energy transfer (LET) (80 keV/μm), causing less toxicity to neighbouring healthy tissues (Pandit-Taskar 2019). However, α-TRT radiopharmaceuticals cannot be used directly for imaging applications for assessing biodistribution and target binding capacity as crucial criteria for patient selection and dose calculation in the clinical setting due to the lack of photons suitable for in vivo imaging (Gallivanone 2017). The development and application of radiopharmaceuticals combining targeted imaging and therapy, also called radiotheranostics, represent a rapidly evolving field in oncologic nuclear medicine (Srivastava 2012; Qaim et al. 2018). Ideal radiotheranostics use different radioisotopes of the same chemical element for imaging and therapy to ensure similar pharmacokinetics, metabolism and biodistribution patterns (Li et al. 2020; Srivastava 2012). Typical examples of ideal radionuclide pairs for radiotheranostics reported in the literature include ^{64}Cu/^{67}Cu, ^{86}Y/^{90}Y, ^{124}I/^{131}I, ^{152} Tb/^{161} Tb, ^{133}La/^{135}La and ^{203}Pb/^{212}Pb (Nelson et al. 2020; Nelson et al. 2023; Kokov et al. 2022; McNeil et al. 2021). In addition, physical half-life, availability, and production costs also require special consideration in the design and development of radiotheranostics (Srivastava 2013).

The ^{203}Pb/^{212}Pb radionuclide pair has recently gained much attention for developing radiotheranostics for TRT (Nelson et al. 2023; Kokov et al. 2022). ^{203}Pb emits γ-photons through electron capture, allowing detection with single-photon emission computed tomography (SPECT) for diagnostic imaging, whereas ^{212}Pb decays by emitting β^--particles and α-particles suitable for delivering therapeutic doses of radiation to cancer cells (Kokov et al. 2022; McNeil et al. 2021).

Targeting vectors in radiotheranostics for TRT encompass small molecules, peptides, antibodies, and nanoparticles (Kerr et al. 2022). Among the targeting vector landscape, monoclonal antibodies (mAb) display exceptional target specificity, making mAb excellent candidates for TRT.

However, their relatively high molecular weight (~ 150 kDa) results in a long biological half-life (slow distribution and elimination profile), which must be matched with a compatible physical half-life of the radionuclide (Mammatas et al. xxxx). Several radiolabelled mAb and antibody fragments are tested in preclinical studies for clinical translation of radioimmunotherapy (RIT), demonstrating promising results for targeting cancer biomarkers epidermal growth factor receptor (EGFR), prostate-specific membrane antigen (PSMA), and human epidermal growth factor receptor 2 (HER2) (Parakh et al. 2022; Chamarthy et al. 2011). The relatively short 10.5 h physical half-life of ^{212}Pb represents particular challenges for targeted RIT, which can be addressed by pretargeting concepts or using smaller immunoconjugates with shorter biological half-lives like antibody fragments (Jiao et al. 2023). However, the efficacy of RIT with ^{212}Pb using full-length antibodies was recently demonstrated with a ^{212}Pb-labeled antibody targeting melanin in a preclinical melanoma model (Bauer et al. 2024).

Panitumumab is an FDA-approved human monoclonal antibody specific to EGFR used as a single drug or in combination with other drugs to treat certain types of colorectal cancer (CRC), especially for the treatment of metastatic colorectal carcinoma with disease progression. Panitumumab binds to the extracellular domain of the EGFR, preventing EGFR dimerization, thus, halting ligand-induced receptor autophosphorylation and intracellular signalling pathway activation (Gemmete and Mukherji 2011). EGFR is overexpressed in many solid tumour cancers, including CRC, head and neck squamous cell carcinoma (HNSCC), non-small cell lung cancer (NSCLC) and breast cancer (Thomas and Weihua 2019; Rogers et al. 2005). Several studies demonstrated the relationship between EGFR overexpression and survival rate in these cancers: as EGFR expression increased, survival decreased (Braun et al. 2018), making EGFR a promising target for TRT of solid tumours.

Herein we describe the radiolabelling of panitumumab with ^{203}Pb using novel bifuntional chelating agent 2,2'-(4-(2-amino-2-oxoethyl)-10-(2-((4-isothiocyanatobenzyl) amino)-2-oxoethyl)-1,4,7,10 tetraazacyclododecane-1,7-diyl) diacetic acid (PSC-NCS) (Nelson et al. 2023). Immuno-SPECT radioligand ^{203}Pb-PSC-panitumumab was evaluated using SPECT and biodistribution studies in NRG mice bearing subcutaneous (s.c.) HNSCC patient-derived xenografts (PDX). Our work using ^{203}Pb-PSC-panitumumab provides critical data for developing and testing ^{212}Pb-PSC-panitumumab for future TRT applications using $^{203/212}$Pb-PSC-panitumumab radiotheranostics.

Materials and methods

Production of ^{203}Pb

^{203}Pb was produced using a recently published procedure (Nelson et al. 2023). Briefly, ^{205}Tl metal (99.9% isotopic enrichment) targets were irradiated at 23.3 MeV on a TR-24 cyclotron at currents up to 60 μA to produce ^{203}Pb via the ^{205}Tl(p,3n)^{203}Pb nuclear reaction. Following a cool-down period of > 12 h, targets were removed and irradiated ^{205}Tl dissolved in 4 M HNO_3. A NEPTIS Mosaic-LC synthesis unit performed automated separation using Eichrom Pb resin, and ^{203}Pb was eluted using 8 M HCl or 1 M NH_4OAc. Purified ^{203}Pb yields of up to 12 GBq were attained (15.8 GBq at EOB). The [^{203}Pb]$PbCl_2$ and [^{203}Pb]$Pb(OAc)_2$ products contained no detectable radionuclidic impurities besides

^{201}Pb (< 0.1%), and < 0.4 ppm stable Pb. ^{205}Tl metal was recovered with a 92% batch yield (Nelson et al. xxxx).

Preparation of ^{203}Pb-PSC-panitumumab radioimmunoconjugate

General

All glassware was rinsed with ultra-pure HCl (Fisherbrand, A508-P500). Trace metal-based ultra-pure chemicals for buffer preparations were purchased from Sigma Aldrich. All buffer solutions were treated with biotechnology-grade Chelex 100 (Bio-Rad, 143–2832).

PSC functionalization of panitumumab and radiolabeling with [^{203}Pb]Pb(OAc)$_2$

2,2'-(4-(2-amino-2-oxoethyl)-10-(2-((4-isothiocyanatobenzyl)amino)-2-oxoethyl)-1,4,7,10-tetra-azacyclododecane-1,7-diyl) diacetic acid (PSC-NCS) chelator (Li et al. 2023) (200 µg) was dissolved in 50 µL of 0.1 M $NaHCO_3$ (pH = 9.0) and added to 400 µL of panitumumab (Vectibex ® 20 mg/mL). The pH was adjusted to 8.0 and left on a thermoshaker set at 800 rpm and 30 °C for 2.5 h.

The samples were purified via size exclusion chromatography (Bio-Rad 10DG desalting column, USA), which was pre-equilibrated and eluted with 0.025 M NaOAc buffer (pH = 5.5). The antibody concentration of each fraction was measured using a nanodrop spectrophotometer (Thermo Scientific, NanoDrop OneC), and the fraction with the highest protein concentration was submitted for analysis via matrix-assisted laser desorption/ionization (MALDI) to assess the number of PCS chelators per antibody (~ 5 chelators per antibody). [^{203}Pb]Pb(OAc)$_2$ (150–200 MBq) was added to PSC-panitumumab (200 µg), and the reaction was kept at room temperature for 5–10 min at pH = 5.

Radio-thin layer chromatography (radio-TLC) analysis (AR-2000, Eckert and Ziegler) was used to determine ^{203}Pb incorporation efficiency by spotting samples on silica plates and using 20 mM EDTA and 0.2 M NaOAc as the mobile phase; in this system, the R_f for [^{203}Pb]Pb(OAc)$_2$ was1.0 and for ^{203}Pb-PSC-panitumumab will be zero (McNeil et al. 2021). ^{203}Pb-PSC-panitumumab was purified on an Econo-Pac 10DG desalting column pre-equilibrated with 0.25 M sodium acetate, pH 5.5 used as the eluant.

Elution fractions (300 µL) were collected from the column, and the radioactivity was measured using an Atomlab 400 dose calibrator (Biodex, Shirley, NY, USA). Laemmli buffer (Bio-Rad, USA) was added to ^{203}Pb-PSC-panitumumab, and the samples (15 µL) were incubated at 95 °C for 5 min. Then, the samples were loaded on SDS-PAGE (Bio-Rad, Mini-PROTEAN® TGX™ Precast Protein Gels) and ran at 120 V. The gel was imprinted on film and evaluated by autoradiography on a BAS-5000 phosphor imager (Fujifilm).

Functional characterization of ^{203}Pb-PSC-panitumumab

Cell uptake studies

EGFR-expressing neck and neck cancer FaDu cells were cultured in a 5% CO_2 incubator at 37 °C in Gibco DMEM media supplemented with 10% fetal bovine serum (Gibco, USA) and 1% penicillin/streptomycin with media renewal 2–3 times per week. For cellular uptake studies, 200,000 cells per well were seeded in 6-well plates and left in the incubator overnight. The media was removed, and 500 µL of Kerbs-Ringer

buffer solution (Bailey and Ong 1978) was added to each well, followed by the addition of 0.2 MBq of ^{203}Pb-PSC-panitumumab, and the plate was kept in the incubator at 37 °C at 5% CO_2. Cell uptake was terminated at 1, 5, 15, 30, 45, 60, and 90 min by adding ice-cold Krebs buffer (120 mM NaCl, 4 mM KCl, 1.2 mM KH_2PO_4, 2.5 mM, $MgSO_4$, 25 mM $NaHCO_3$, 70 µM $CaCl_2$, pH 7.4) and rinsing the wells twice to wash away unbound radioimmunoconjugates before lysing the cells with RIPA buffer. The cell lysates were transferred to scintillation vials and measured for radioactivity using a γ-counter (Wizard2® 2480 Automatic Gamma Counter, Perkin-Elmer, Canada). In addition, according to the manufacturer's recommendations, protein levels in each sample was quantified using a Pierce™ BCA protein assay kit. For blocking studies, the FaDu cells were co-treated with different amounts of unlabeled panitumumab (0.5–10 µg) and 0.2 MBq of ^{203}Pb-PSC-panitumumab. Cell uptake levels were normalized to percent of the total amount of radioactivity per milligram of protein (% radioactivity/mg protein) and plotted as a function of time. All experiments were performed in triplicates.

Immunoreactivity

The immunoreactivity of ^{203}Pb-PSC-panitumumab was assessed by a cell binding assay with EGFR-expressing FaDu cells using the Lindmo et al. method (Lindmo et al. 1984). 0.25, 0.5, 1, 2, 3, 4, and 5×10^6 FaDu cells were disperesed in 500 µL of PBS supplemented with 1% bovine serum albumin (Sigma, USA). Then, 20,000 cpm of ^{203}Pb-PSC-panitumumab was added to each cell concentration. The samples were placed on a rocker for one hour at room temperature. After triplicate PBS washes, the samples were transferred to 1.5 mL LoBind® tubes (Eppendorf, USA), and by using a γ-counter (Wizard2® 2480 Automatic Gamma Counter, Perkin-Elmer, Canada), the counts of each sample were determined.

The radioactivity data obtained was corrected in the background and compared to counts from the total activity added to control samples in the experiments. The immunoreactive fraction was calculated by performing a linear regression analysis on a double-inverse plot of (total/bound) activity *versus* normalized cell concentration.

In vivo *experiments*

Xenograft models

A primary tumour specimen (#391) was surgically obtained from a patient with HNSCC under a protocol approved by the Research Ethics Board at the University Health Network (Protocol No. 12–5639). This tumour was dissected into small fragments (~ 1 mm^3) and engrafted subcutaneously (s.c.) on the right flank of NOD Rag2 γc (NRG) immunodeficient male mice (3–4 months old). These patient-derived tumour xenografts (PDX) were serially propagated in NRG mice following an Animal Care Protocol (No. 1542.28) approved by the Animal Care Committee at the University Health Network and following Canadian Council on Animal Care guidelines. The PDX used in this study was between the 3rd to 5th passage from the initial engraftment of the HNSCC tumour in NRG mice.

SPECT/CT imaging

NRG mice were anesthetized using 2% isoflurane in O_2, and microSPECT/CT images were acquired in a supine position at 48 h and 120 h on a NanoScan® SPECT/CT/PET system (Mediso). Either ^{203}Pb-PSC-panitumumab or ^{203}Pb-DOTA-panitumumab-NPs (~10 MBq; 140 µL) were injected into the tail vein of NRG mice engrafted with subcutaneous HNSCC PDX. Mice were divided into two study groups: A group of mice (n = 3), was only injected with ^{203}Pb-PSC-panitumumab, and the blocking group (n = 3) was injected with 1 mg of panitumumab 1 h before administration of ^{203}Pb-PSC-panitumumab to block EGFR. SPECT/CT images were acquired 48 and 120 h post-injection (p.i.) of the radioligand. Images were acquired in a 256 × 256 matrix.

A Mediso APT62 collimator (WB-HS standard) was affixed to each of the four detector NaI (TI) detector heads. Images were reconstructed by Monte Carlo methods with three subsets of data undergoing 48 iterations using the Mediso Nucline NanoScan acquisition and reconstruction software (ver 3.00.020.0000). Before SPECT imaging, CT images were acquired with 50 kVp X-rays, 980 µA and a 300 ms exposure time. CT scans were reconstructed using the medium voxel and slice thickness settings, resulting in an isotropic voxel size of 250 µm. SPECT and CT were co-registered by the Mediso Nucline acquisition/reconstruction software. All animal studies were conducted under a protocol (AUP 2843.14) approved by the Animal Care Committee at the University Health Network following the Canadian Council on Animal Care guidelines.

Biodistribution studies

Mice were euthanized five days (120 h) after the injection of ^{203}Pb-PSC-panitumumab, and tissues and organs were collected, weighed, and radioactivity was counted in a γ-counter. The uptake was calculated as injected dose percentage per gram of each tissue (ID%/g). Two groups were studied for biodistribution experiments: (1) Mice (n = 5) injected with ^{203}Pb-PSC-panitumumab, and (2) Mice (n = 3) were injected with 1 mg of panitumumab one hour before the injection of ^{203}Pb-PSC-panitumumab to block EGFR.

Statistical analysis

All data are expressed as means ± SEM. Graphs were constructed using GraphPad Prism 4.0 (GraphPad Software). Where applicable, statistical differences were tested by unpaired Student's *t*-test and were considered significant for $p < 0.05$.

Results

Radiochemistry

MALDI analysis confirmed the conjugation of 4–5 PSC chelators per antibody by reacting the isothiocyanate group in PSC-NCS with lysine residues in panitumumab (Fig. 1A). PSC-conjugated panitumumab was used for radiolabeling with [^{203}Pb]Pb$(OAc)_2$, and the radiolabelling efficiency was measured with radio-TLC, indicating 99.2 ± 0.7% incorporation of $^{203}Pb^{2+}$ (Fig. 1B and 1C) which is comparable to results obtained by Nelson et al. (Nelson et al. 2023). SDS-PAGE analysis further confirmed incorporation of ^{203}Pb to panitumumab. Reductive SDS-PAGE conditions resulted in the formation of

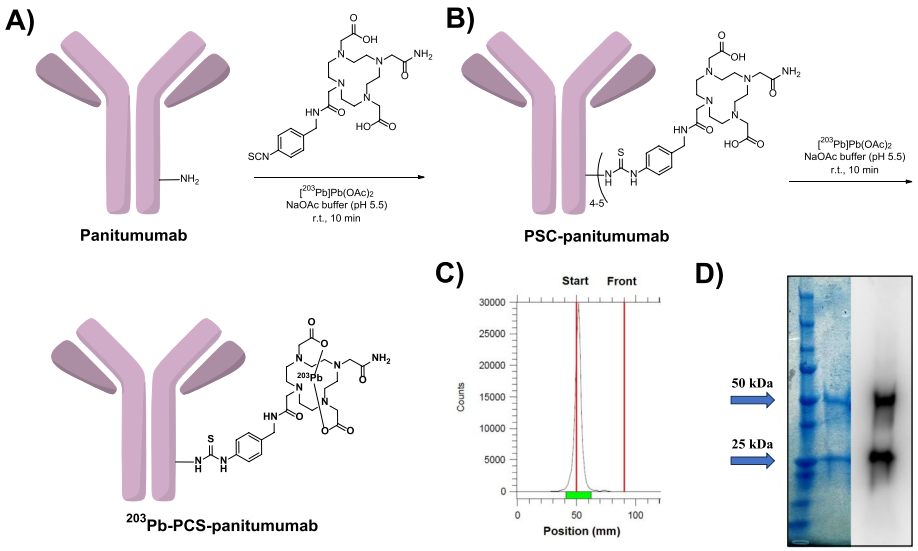

Fig. 1 Synthesis and radiolabeling of PSC-conjugated panitumumab with ^{203}Pb (**A** and **B**) and measurement of $^{203}Pb^{2+}$ incorporation efficiency and radiochemical purity of purified ^{203}Pb-PSC-panitumumab by radio-TLC (**C**) and SDS-PAGE (**D**)

panitumumab light and heavy chains, which were visible at 25 and 50 kDa, respectively, indicating that both antibody portions were modified with the PSC chelator and labelled with ^{203}Pb (Fig. 1D).

^{203}Pb-labeling and purification of radioimmunoconjugate ^{203}Pb-PSC-panitumumab provided isolated radiochemical yields of 41.5 ± 8% (n = 5) at a molar activity of 1.2 ± 0.35 GBq/mg. The radiochemical purity of the isolated radioimmunoconjugates was greater than 99%, as analyzed by radio-TLC. Purified radioimmunoconjugates were > 95% stable in human serum over 48 h.

Cellular uptake of ^{203}Pb-PSC-panitumumab

EGFR-expressing FaDu cells were incubated with ^{203}Pb-PSC-panitumumab, and cell uptake was measured at different time points. ^{203}Pb-PSC-panitumumab uptake in FaDu cells increased until it reached a plateau at 60 min (Fig. 2A). EGFR specificity of cellular uptake was confirmed with blocking studies using different amounts of panitumumab (0.5 µg–10), demonstrating 70%, 85%, and 95% blocking at 0.5 µg, 1 µg, 5 µg and 10 µg, respectively (Fig. 2B). The immunoreactive fraction of ^{203}Pb-PSC-panitumumab was found to be ~ 30%, which is lower than the reported 68% for ^{89}Zr-labelled panitumumab measured in MDA-MB-468 cells (Bhattacharyya et al. 2013) (Fig. 2C).

In vivo imaging (microSPECT/CT)

MicroSPECT/CT images were acquired to visualize the biodistribution of ^{203}Pb-PSC-panitumumab in NRG mice bearing subcutaneous EGFR + HNSCC PDX tumours (Fig. 3). EGFR specificity was tested with in vivo blocking studies by administering 1 mg of panitumumab before ^{203}Pb-PSC-panitumumab injection to block EGFR (n = 3). SPECT images were taken at two time points of 48 and 120 h p.i. of ^{203}Pb-PSC-panitumumab to monitor changes in tumour uptake and distribution of

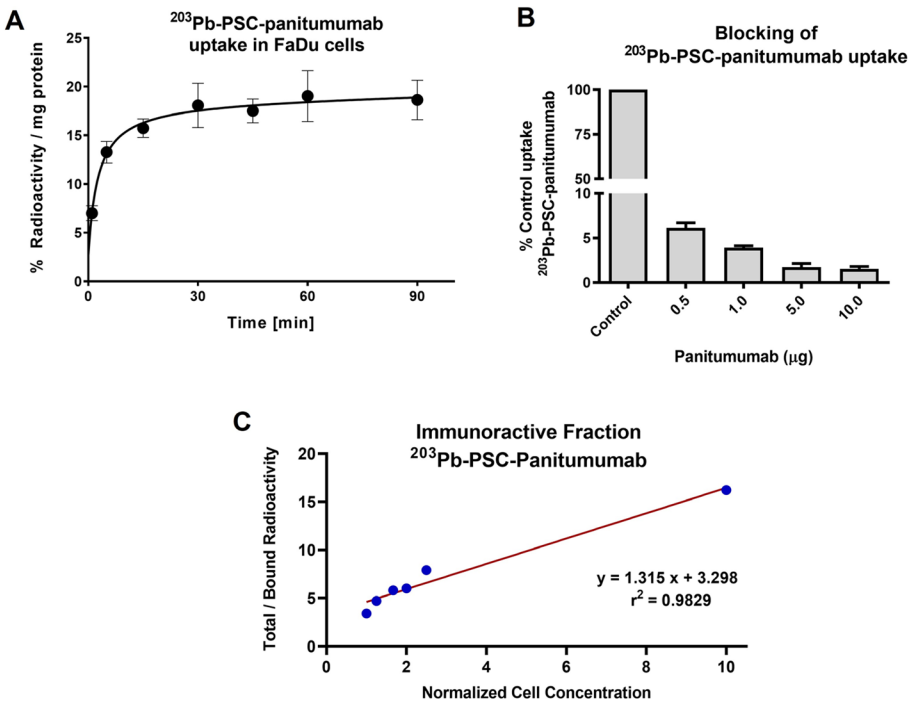

Fig. 2 Cellular uptake of ^{203}Pb-PSC-panitumumab uptake in EGFR + FaDu cells (**A**) and studies of ^{203}Pb-PSC-panitumumab binding competed with increasing amounts of panitumumab (**B**). Representative double inverse plot from Lindmo assay performed in FaDu cells with ^{203}Pb-PSC-panitumumab (**C**)

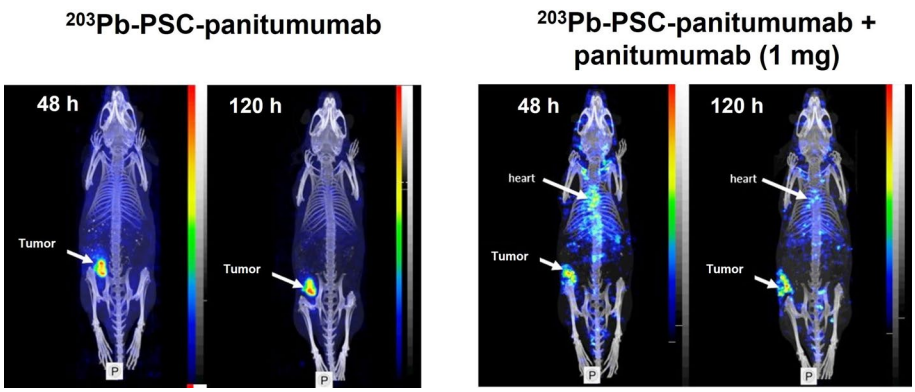

Fig. 3 Representative SPECT/CT images of NRG mice engrafted with EGFR + HNCC PDX at 48 and 120 h p.i. under control and blocking conditions. Tumours are highlighted with an arrow

^{203}Pb-PSC-panitumumab over time. The tumours were clearly visible in SPECT/CT images at both time points without significant radioactivity in other organs and tissues (Fig. 3).

Under EGFR blocking conditions, SPECT/CT images after 48 h and 120 h indicated lower tumour uptake and somewhat increased radioactivity in the heart and blood pool. The remaining radioactivity observed in the tumour under blocking conditions at 48 and 120 h is presumably due to the EPR effect, as typically found in immunoPET and immunoSPECT experiments with solid tumours (Dewulf et al. 2020).

Biodistribution studies

NRG mice bearing EGFR + PDX HNCC tumours were euthanized at 120 h p.i. either after ^{203}Pb-PSC-panitumumab (n = 5) or 1 mg of panitumumab pre-injection with ^{203}Pb-PSC-panitumumab (n = 5). The results (Table 1) indicated that baseline tumour uptake at 120 h p.i. was significantly higher (26 ± 07 ID%/g) than in all other organs reaching tumour-to-blood (T/B) and tumour-to-muscle (T/M) radios of 4.2 and 37.3, respectively.

Tumour uptake could be significantly reduced (6.2 ± 1.0 ID%/g ($p < 0.05$)) in mice pretreated with an excess panitumumab (1 mg) one hour before radiotracer administration. In mice pretreated with panitumumab, tumour uptake was comparable to that of the blood at 120 min p.i. as represented by a T/B ratio of 0.94 at 120 h p.i. The remaining radioactivity in the tumour under EGFR-blocking conditions can be attributed to the EPR effect.

Discussion

EGFR + HNCC accounts for almost 90% of HNCC cases diagnosed in the clinic (Fasano et al. 2021). This expression offers EGFR as a suitable receptor to target head and neck cancer cells when developing radiotheranostics for HNCC. Creating a radiotheranostic pair using radionuclides of the same chemical element that targets EGFR provides a probe for imaging and treatment with similar pharmacokinetics, leading to similar biodistribution in EGFR + tumours (Li et al. 2020; Srivastava 2012).

As in the presented work, the uptake and biodistribution of ^{203}Pb-PSC-panitumumab was studied in vitro on EGFR + HNCC FaDu cells as well as in mice bearing patient-derived xenografts which were taken from patients with EGFR + HNCC.

Immuno-SPECT probe ^{203}Pb-PSC-panitumumab displayed EGFR-mediated uptake in vitro and in vivo with high tumour retention, enabling the detection of tumours at

Table 1 Biodistribution of ^{203}Pb-PSC-panitumumab at 120 h p.i

Tissue	Percent injected dose per gram (mean ± SEM)	
	^{203}Pb-PSC panitumumab	^{203}Pb-PSC panitumumab + panitumumab (1 mg)
Blood	6.2 ± 1.2	6.6 ± 2.4
Heart	1.8 ± 0.6	1.7 ± 0.6
Lung	2.5 ± 0.8	3.2 ± 1.7
Liver	2.5 ± 0.8	2.1 ± 0.3
Kidney	1.8 ± 0.4	2.1 ± 0.7
Spleen	3.1 ± 0.5	3.2 ± 2.2
Pancreas	0.7 ± 0.2	0.5 ± 0.2
Stomach	0.7 ± 0.2	0.6 ± 0.3
Intestine	0.5 ± 0.1	0.5 ± 0.3
Muscle	0.7 ± 0.3	0.7 ± 0.3
Bone	1.1 ± 0.3	0.9 ± 0.4
Skin	1.3 ± 0.5	1.4 ± 0.4
Brain	0.1 ± 0.0	0.2 ± 0.1
Tumour	26.1 ± 1.2	6.2 ± 1.0
T/B ratio	4.2	0.94
T/M ratio	37.3	8.8

48 h and 120 h p.i.. Previous reports in the literature for radiolabelling panitumumab with SPECT-detectable radioisotopes were labelling with ^{111}In (Facca et al. 2023) and ^{177}Lu (Aghevlian et al. 2018); also, the Fab fragment of panitumumab was labelled with ^{177}Lu (Ku et al. 2021) and ^{99m}Tc (Ku et al. 2019); however, no previous studies describing labelling panitumumab with ^{203}Pb were reported. Antibody-based compounds such as trastuzumab (Herceptin) via DOTA (Garmestani et al. 2005), c8C3 via TCMC (Jiao et al. 2023), and peptides such as α-melanocyte-stimulating hormone (Miao et al. 2008), and low molecular weight PSMA ligands (Banerjee et al. 2020) have been labelled with ^{203}Pb using DOTA coordination chemistry. Also, the conditions required for labelling panitumumab with ^{111}In using diethylenetriamine-pentaacetic acid (DTPA) and/or ^{89}Zr using *p*-isothiocyanatobenzyl-desferrioxamine B included heating to 37 °C, and depending on the chelator administered, different reaction times of up to 4 h were required (Ray et al. 2009; Nayak et al. 2012). Moreover, high temperatures (60–75 °C) were reported for the radiolabelling of peptides with ^{203}Pb to achieve high incorporation efficiency with shorter incubation times (Liu et al. 2014; Nayak et al. 2010). However, in the presented work, the PSC-NCS chelator labelling process did not require any elevated temperatures, and $^{203}Pb^{2+}$ incorporation proceeded with high efficiency (> 99%) at short reaction times of 5–10 min at room temperature. The observed high labelling efficiency > 99 aligns with previously reported data using PSC-NCS as a lead-specific bifunctional chelating agent for rapid coordination chemistry with $^{203}Pb^{2+}$ under mild conditions (Nelson et al. 2023).

Figure 1D indicates that both light and heavy chains of panitumumab are labelled with ^{203}Pb, confirming the bioconjugation of lysine residues through thiourea formation with the PSC-NCS chelator being present in both light and heavy chains of panitumumab (Ho 2023). Modifying both heavy and light chains of panitumumab can also explain the only moderate immunoreactivity of ~ 30% (Fig. 2C). However, ^{203}Pb-PSC-panitumumab still provided clear SPECT images for detecting EGFR + HNSCC PDX tumours.

The specific binding to EGFR was confirmed by blocking studies by pre-administering an excess of panitumumab. Also, ^{203}Pb-PSC-panitumumab allowed for imaging to be conducted at several time points for SPECT/CT imaging by remaining in the tumour up to 120 h post-injection in tumour-bearing mice. Our findings indicate that ^{203}Pb-PSC-panitumumab is a suitable SPECT probe with desirable biodistribution for EGFR + HNCC. ^{203}Pb-PSC-panitumumab was taken up by FaDu cells, and the uptake could be reduced under blocking conditions in a concentration-dependent manner using panitumumab. Indicating that the cell uptake of 203Pb-PSC-panitumumab is receptor mediated and not affected by PSC chelators. SPECT/CT images acquired from tumour-bearing mice after the injection of ^{203}Pb-PSC-panitumumab allowed clear delineation of the tumour tissue, confirming high tumour uptake and retention of the radioligand in the EGFR + HNSCC PDX model.

Our work aligns with reported PET and SPECT data in mice using ^{89}Zr-, ^{177}Lu- and ^{111}In-labelled panitumumab immunoconjugates (Ray et al. 2009; Nayak et al. 2012; Liu et al. 2014), confirming that radioligand ^{203}Pb-PSC-panitumumab is a suitable immuno-SPECT probe for detecting EGFR + tumours. The long physical half-life of ^{203}Pb ($t_{1/2}$ = 51.9 h) allows SPECT imaging protocols for several days at a high image quality.

The biodistribution data (%ID/g) in tissues and organs confirmed the SPECT/CT data in mice injected with ^{203}Pb-PSC-panitumumab. The highest radioactivity was measured

in tumours (26.1 ± 1.2) after 120 p.i. of ^{203}Pb-PSC-panitumumab, which is comparable to the radioactivity accumulation and retention in reported for LS-174 T, SHAW and SKOV-3 xenografts using ^{111}In-CHX-A"-DTPA-panitumumab (Ray et al. 2009; Chopra 2004) and MDA-MB-468 xenografts using ^{89}Zr-labelled panitumumab (Nayak et al. 2012). The observed biodistribution pattern was also similar to a study using ^{86}Y-CHX-A"-DTPA-panitumumab in EGFR + human colorectal, prostate, and epidermoid tumour xenografts (Nayak et al. 2010). Radioactivity uptake in EGFR + HNSCC PDX could be reduced by ~ 75% by predosing mice with panitumumab (1 mg), confirming EGFR-mediated uptake of radioligand ^{203}Pb-PSC-panitumumab. As panitumumab is a human antibody against human EGFR it does not bind to mouse EGFR; therefore, administering an excess of panitumumab before injecting ^{203}Pb-PSC-panitumumab will only block EGFR on the tumour. The remaining radioactivity amount (6.24 ± 0.97%ID/g) can be attributed to the EPR effect commonly observed during SPECT and PET imaging in solid tumours using radiolabeled immunoconjugates (Sharma et al. 2014).

Our work with ^{203}Pb-PSC-panitumumab as a novel immuno-SPECT probe highlights the opportunity for developing $^{203/212}$Pb-PSC-panitumumab as ideal radiotheranostics for combined SPECT imaging and targeted alpha therapy of EGFR-expressing cancers. $^{203/212}$Pb radiotheranostics represent an attractive alternative to currently used ^{225}Ac-based radiotheranostics for targeted alpha therapy.

The availability of ^{212}Pb through the emerging ^{224}Ra/^{212}Pb generator technology and the ideal radionuclide matching pair characteristics of radiometals ^{203}Pb and ^{212}Pb ensure identical coordination chemistry and identical biodistributions profiles of $^{203/212}$Pb radiotheranostics. This represents a significant advantage to currently used ^{225}Ac-based radiotheranostics for targeted alpha therapy, which rely on chemically different imaging surrogates, such as ^{133}La and ^{134}Ce, as no Ac isotopes are available suitable for imaging (Nelson et al. 2023).

Conclusion

In this study, panitumumab was successfully modified with PSC-NCS as a novel Pb-specific bifunctional chelating agent. PSC-decorated human antibody panitumumab was rapidly and reproducibly radiolabelled with ^{203}Pb(OAc)$_2$ in good radiochemical yields under mild reaction conditions compatible with the structural and functional integrity of an antibody. Novel immunoSPECT probe ^{203}Pb-PSC-panitumumab showed EGFR-mediated uptake in FaDu cells and high uptake and retention in an EGFR + HNSCC PDX model. EGFR-mediated uptake was confirmed by SPECT/CT and biodistribution studies using blocking experiments with panitumumab. Our work introduces ^{203}Pb-PSC-panitumumab as a novel immuno-SPECT probe for imaging EGFR + tumours and an opportunity to develop $^{203/212}$Pb-PSC-panitumumab radiotheranostics for combined SPECT imaging and targeted alpha therapy of EGFR-expressing cancers.

Acknowledgements

Nasim Sarrami expresses gratitude for the NSERC-CREATE "Polymer Nanoparticles for Drug Delivery (PoND)" program, Alberta Innovates, and Graduate scholarships from the Faculty of Pharmacy and Pharmaceutical Sciences of the University of Alberta. The authors thank the Cross Cancer Institute pharmacy for generously gifting Vectibex®.

Author contributions

NS was responsible for the synthesis of ^{203}Pb-PSC-panitumumab, cell-based experiments and SPECT imaging and writing the manuscript; BN, SM, JW, and MS were responsible for preparing ^{203}Pb and PSC-NCS; CC, JM, TK, LA contributed to the PDX-model experiments, SPECT imaging and biodistribution; MW contributed to data analysis, AL, RR, LA and FW

edited and revised the manuscript. FW and RR were responsible for the design of the study and critically reviewed the manuscript; and all authors read and approved the final manuscript and agreed to be accountable for the integrity of the work.

Funding
The work was supported by a New Frontiers in Research Fund-Transformation grant with funds from the Government of Canada and the Dianne and Irving Kipnes Foundation.

Availability of data and materials
Not applicable.

Declarations

Ethics approval and consent to participate
All experimental protocols were approved by the Research Ethics Board at the University Health Network (Protocol No. 12–5639). All methods were performed per the ethical standards laid down in the Declaration of Helsinki and its later amendments or comparable ethical standards.

Consent for publication
Not applicable.

Competing interests
All authors declare no competing financial or non-financial interests.

Received: 20 August 2024 Accepted: 15 November 2024
Published online: 26 November 2024

References

Aghevlian S, Lu Y, Winnik MA, Hedley DW, Reilly RM. Panitumumab modified with metal-chelating polymers (MCP) complexed to ^{111}In and ^{177}Lu–an EGFR-targeted theranostic for pancreatic cancer. Mol Pharmaceutics. 2018;15(3):1150–9.
Bailey LE, Ong SD. Krebs-Henseleit solution as a physiological buffer in perfused and superfused preparations. J Pharmacol Methods. 1978;1(2):171–5.
Banerjee SR, Minn I, Kumar V, Josefsson A, Lisok A, Brummet M, et al. Preclinical evaluation of $^{203/212}$Pb-labeled low-molecular-weight compounds for targeted radiopharmaceutical therapy of prostate cancer. J Nucl Med. 2020;61(1):80–8.
Bauer D, Carter LM, Atmane MI, De Gregorio R, Michel A, Kaminsky S, Monette S, Li M, Schultz MK, Lewis JS. 212Pb-pretargeted theranostics for pancreatic cancer. J Nucl Med. 2024;65(1):109–16.
Bhattacharyya S, Kurdziel K, Wei L, Riffle L, Kaur G, Hill GC, et al. Zirconium-89 labeled panitumumab: a potential immuno-PET probe for HER1-expressing carcinomas. Nucl Med Biol. 2013;40(4):451–7.
Braun AC, de Mello CAL, Corassa M, Abdallah EA, Urvanegia AC, Alves VS, et al. EGFR expression in circulating tumor cells from high-grade metastatic soft tissue sarcomas. Cancer Biol Ther. 2018;19(6):454–60.
Chamarthy MR, Williams SC, Moadel RM. Radioimmunotherapy of non-Hodgkin's lymphoma: from the "magic bullets" to "radioactive magic bullets." Yale J Biol Med. 2011;84(4):391–407.
Chan TG, O'Neill E, Habjan C, Cornelissen B. Combination strategies to improve targeted radionuclide therapy. J Nucl Med. 2020;61(11):1544–52.
Chopra A. 111In-Labeled panitumumab, a fully human monoclonal antibody directed against the extracellular domain III of the epidermal growth factor receptor. In: Molecular Imaging and Contrast Agent Database (MICAD) [Internet]. Bethesda (MD): National Center for Biotechnology Information (US); 2004 [cited 2024 Jan 17]. Available from: http://www.ncbi.nlm.nih.gov/books/NBK97967/
Dewulf J, Adhikari K, Vangestel C, Wyngaert TVD, Elvas F. Development of antibody immuno-PET/SPECT radiopharmaceuticals for imaging of oncological disorders—an update. Cancers. 2020;12(7):1868.
Facca VJ, Cai Z, Ku A, Georgiou CJ, Reilly RM. Adjuvant auger electron-emitting radioimmunotherapy with [111 In] In-DOTA-panitumumab in a mouse model of local recurrence and metastatic progression of human triple-negative breast cancer. Mol Pharmaceutics. 2023;20(12):6407–19.
Fasano M, Della Corte CM, Viscardi G, Di Liello R, Paragliola F, Sparano F, et al. Head and neck cancer: the role of anti-EGFR agents in the era of immunotherapy. Ther Adv Med Oncol. 2021;13:175883592094941.
Gallivanone F. Targeted radionuclide therapy frontiers in theranostics. Front Biosci. 2017;22(10):1750–9.
Garmestani K, Milenic DE, Brady ED, Plascjak PS, Brechbiel MW. Purification of cyclotron-produced 203Pb for labeling Herceptin. Nucl Med Biol. 2005;32(3):301–5.
Gemmete JJ, Mukherji SK. Panitumumab (Vectibix): Fig 1. AJNR Am J Neuroradiol. 2011;32(6):1002–3.
Gill MR, Falzone N, Du Y, Vallis KA. Targeted radionuclide therapy in combined-modality regimens. Lancet Oncol. 2017;18(7):e414–23.
Ho FKS. Development of 197Hg-Labelled Panitumumab for Auger Electron Radioimmunotherapy of Triple-Negative Breast Cancer [Internet] [M.Sc.]. ProQuest Dissertations and Theses. [Canada-Ontario, CA]: University of Toronto (Canada); 2023. Available from: https://login.ezproxy.library.ualberta.ca/login?url=https://www.proquest.com/dissertations-theses/development-sup-197-hg-labelled-panitumumab-auger/docview/2889518073/se-2?accountid=14474

Jiao R, Allen KJH, Malo ME, Yilmaz O, Wilson J, Nelson BJB, Wuest F, Dadachova E. A theranostic approach to imaging and treating melanoma with 203Pb/212Pb-labeled antibody targeting melanin. Cancers (Basel). 2023;15(15):3856.
Jiao R, Allen KJH, Malo ME, Yilmaz O, Wilson J, Nelson BJB, et al. A theranostic approach to imaging and treating melanoma with 203Pb/212Pb-labeled antibody targeting melanin. Cancers. 2023;15(15):3856.
Kerr CP, Grudzinski JJ, Nguyen TP, Hernandez R, Weichert JP, Morris ZS. Developments in combining targeted radionuclide therapies and immunotherapies for cancer treatment. Pharmaceutics. 2022;15(1):128.
Kokov KV, Egorova BV, German MN, Klabukov ID, Krasheninnikov ME, Larkin-Kondrov AA, et al. 212Pb: production approaches and targeted therapy applications. Pharmaceutics. 2022;14(1):189.
Ku A, Chan C, Aghevlian S, Cai Z, Cescon D, Bratman SV, et al. MicroSPECT/CT imaging of cell-line and patient-derived EGFR-positive tumor xenografts in mice with panitumumab fab modified with hexahistidine peptides to enable labeling with ^{99m}Tc(I) tricarbonyl complex. Mol Pharmaceutics. 2019;16(8):3559–68.
Ku A, Kondo M, Cai Z, Meens J, Li MR, Ailles L, et al. Dose predictions for [177Lu]Lu-DOTA-panitumumab F(ab′)2 in NRG mice with HNSCC patient-derived tumour xenografts based on [64Cu]Cu-DOTA-panitumumab F(ab′)2 – implications for a PET theranostic strategy. EJNMMI Radiopharm Chem. 2021;6(1):25.
Li M, Sagastume EA, Lee D, McAlister D, DeGraffenreid AJ, Olewine KR, et al. 203/212Pb theranostic radiopharmaceuticals for image-guided radionuclide therapy for cancer. CMC. 2020;27(41):7003–31.
Li M, Baumhover NJ, Liu D, Cagle BS, Boschetti F, Paulin G, Lee D, Dai Z, Obot ER, Marks BM, Okeil I, Sagastume EA, Gabr M, Pigge FC, Johnson FL, Schultz MK. Preclinical evaluation of a lead specific chelator (PSC) conjugated to radiopeptides for 203Pb and 212Pb-based theranostics. Pharmaceutics. 2023;15(2):414.
Lindmo T, Boven E, Cuttitta F, Fedorko J, Bunn PA. Determination of the immunoreactive function of radiolabeled monoclonal antibodies by linear extrapolation to binding at infinite antigen excess. J Immunol Methods. 1984;72(1):77–89.
Liu Z, Ma T, Liu H, Jin Z, Sun X, Zhao H, et al. ^{177}Lu-labeled antibodies for EGFR-targeted SPECT/CT imaging and radioimmunotherapy in a preclinical head and neck carcinoma model. Mol Pharmaceutics. 2014;11(3):800–7.
Mammatas LH, Verheul HMW, Hendrikse NH, Yaqub M, Lammertsma AA, Menke-van Der Houven Van Oordt CW. Molecular imaging of targeted therapies with positron emission tomography: the visualization of personalized cancer care. Cell Oncol. 2015; 38(1):49–64.
McNeil BL, Robertson AKH, Fu W, Yang H, Hoehr C, Ramogida CF, et al. Production, purification, and radiolabeling of the 203Pb/212Pb theranostic pair. EJNMMI Radiopharm Chem. 2021;6(1):6.
Miao Y, Figueroa SD, Fisher DR, Moore HA, Testa RF, Hoffman TJ, et al. ^{203} Pb-labeled α-melanocyte–stimulating hormone peptide as an imaging probe for melanoma detection. J Nucl Med. 2008;49(5):823–9.
Nayak TK, Garmestani K, Baidoo KE, Milenic DE, Brechbiel MW. Preparation, biological evaluation, and pharmacokinetics of the human anti- *HER1* monoclonal antibody panitumumab labeled with ^{86}Y for quantitative PET of carcinoma. J Nucl Med. 2010;51(6):942–50.
Nayak TK, Garmestani K, Milenic DE, Brechbiel MW. PET and MRI of metastatic peritoneal and pulmonary colorectal cancer in mice with human epidermal growth factor receptor 1–targeted ^{89}Zr-labeled panitumumab. J Nucl Med. 2012;53(1):113–20.
Nelson BJB, Wilson J, Andersson JD, Wuest F. High yield cyclotron production of a novel 133/135La theranostic pair for nuclear medicine. Sci Rep. 2020;10(1):22203.
Nelson BJB, Wilson J, Andersson JD, Wuest F. Theranostic imaging surrogates for targeted alpha therapy: progress in production, purification, and applications. Pharmaceuticals (Basel). 2023;16(11):1622.
Nelson BJB, Wilson J, Schultz MK, Andersson JD, Wuest F. High-yield cyclotron production of 203Pb using a sealed 205Tl solid target. Nucl Med Biol. 2023;116–117:108314.
Nelson BJB, Wilson J, Schultz MK, Andersson JD, Wuest F. High-yield cyclotron production of 203Pb using a sealed 205Tl solid target. Nucl Med Biol. 2023;116–117:108314.
Pandit-Taskar N. Targeted radioimmunotherapy and theranostics with alpha emitters. J Med Imaging Rad Sci. 2019;50(4):S41–4.
Parakh S, Lee ST, Gan HK, Scott AM. Radiolabeled antibodies for cancer imaging and therapy. Cancers. 2022;14(6):1454.
Qaim SM, Scholten B, Neumaier B. New developments in the production of theranostic pairs of radionuclides. J Radioanal Nucl Chem. 2018;318(3):1493–509.
Ray G, Baidoo K, Wong K, Williams M, Garmestani K, Brechbiel M, et al. Preclinical evaluation of a monoclonal antibody targeting the epidermal growth factor receptor as a radioimmunodiagnostic and radioimmunotherapeutic agent. Br J Pharmacology. 2009;157(8):1541–8.
Rogers SJ, Harrington KJ, Rhys-Evans P, Charoenrat OP, Eccles SA. Biological significance of c-erbB family oncogenes in head and neck cancer. Cancer Metastasis Rev. 2005;24(1):47–69.
Sharma SK, Wuest M, Wang M, Glubrecht D, Andrais B, Lapi SE, et al. Immuno-PET of epithelial ovarian cancer: harnessing the potential of CA125 for non-invasive imaging. EJNMMI Res. 2014;4(1):60.
Srivastava SC. Paving the way to personalized medicine: production of some promising theragnostic radionuclides at brookhaven national laboratory. Semin Nucl Med. 2012;42(3):151–63.
Srivastava SC. A bridge not too far: personalized medicine with the use of theragnostic radiopharmaceuticals. J Postgraduate Med Educ Res. 2013;47(1):31–46.
Sun J, Huangfu Z, Yang J, Wang G, Hu K, Gao M, et al. Imaging-guided targeted radionuclide tumor therapy: from concept to clinical translation. Adv Drug Deliv Rev. 2022;190:114538.
Thomas R, Weihua Z. Rethink of EGFR in cancer with its kinase independent function on board. Front Oncol. 2019;9:800.

Publisher's Note